

## Effect of methotrexate on cerebellar development in infant rats

Akihiko SUGIYAMA<sup>1)\*</sup>, Jing SUN<sup>1)</sup>, Kota UEDA<sup>1)</sup>, Satoshi FURUKAWA<sup>2)</sup> and Takashi TAKEUCHI<sup>1)</sup>

<sup>1)</sup> Laboratory of Veterinary Laboratory Medicine, School of Veterinary Medicine, Faculty of Agriculture, Tottori University, Minami 4-101 Koyama-cho, Tottori, Tottori 680-8553, Japan

<sup>2)</sup> Toxicology and Environmental Science Department, Biological Research Laboratories, Nissan Chemical Industries, Ltd., 1470 Shiraoka, Minamisaitama, Saitama 349-0294, Japan

(Received 14 September 2014/Accepted 19 February 2015/Published online in J-STAGE 5 March 2015)

**ABSTRACT.** Six-day-old rats were treated intraperitoneal injections with methotrexate 1 mg/kg, and the cerebellum was examined. Both the length and width of the vermis decreased in the methotrexate-treated group instead of the control from 4 day after treatment (DAT) onward. A significant reduction in the width of the external granular layer was detected on 2 and 3 DAT in the methotrexate group. By 4 DAT, the width of the external granular layer of the methotrexate group was indistinguishable from the control, and by 8 DAT, it was greater than that of the control. The molecular layer of methotrexate group on 8 and 15 DAT was thinner than that of the control. On 1 DAT, in the methotrexate group, there were many TUNEL and cleaved caspase-3-positive granular cells throughout the external granular layer, and they decreased time-dependently. On 1 DAT, in the methotrexate group, phospho-histone H3-positive cells in the external granular layer were fewer than in the control and tended to increase on 2–4 DAT. The p21-positive-rate of the external granule cells in the MTX group was higher than in the control on 1–4 DAT. These results suggested that methotrexate exposure on postnatal day 6 induces a delay, slowing in the migration of external granular cells to the inner granular layer, attributed to decrease or inhibition in the production of external granular cells that had arisen from apoptosis and the decrease in cell proliferative activity, resulting in cerebellar hypoplasia.

**KEY WORDS:** apoptosis, cerebellar hypoplasia, external granular layer, inhibition of cell proliferation, methotrexate, rat

doi: 10.1292/jvms.14-0475; *J. Vet. Med. Sci.* 77(7): 789–797, 2015

Methotrexate (MTX) is both a folate analogue and a folate antagonist, and it inhibits dihydrofolate reductase, which reduces dihydrofolate to tetrahydrofolate [21, 22]. Because tetrahydrofolate is an essential cofactor in thymidylate synthesis and *de novo* purine synthesis, MTX inhibits DNA synthesis and cell proliferation [11, 20, 27, 29]. Imbalance in DNA precursor pools results in accumulation of DNA strand breaks [25, 28]. MTX exposure was shown to induce apoptosis, and its mechanism is considered to be associated with the up-regulation of p53 and p21 proteins [23, 44], repression of the induction of JNK activity and expression of the CD95 receptor/ligand system [33] and reactive oxygen species [17].

MTX has been used for the treatment of malignancies such leukemia and lymphoma, in children as well as adults [24, 30, 32, 34, 35]. MTX chemotherapy is a major component of preventive central nervous system treatment for childhood acute lymphoblastic leukemia (ALL) [24]. However, several cases of cerebellar toxicity in children during MTX chemotherapy have been reported [5, 24]. Children with ALL treated with MTX, hydrocortisone and cytarabine in combination before 5 years of age had structural anomalies

and dysfunction of cerebellum [24]. Children treated with both MTX chemotherapy and cranial irradiation before the age of 5 years showed cerebellar hypoplasia [5]. However, there are few reports having shown detailed histopathological changes of MTX-induced cerebellar injury in children, and the mechanism of cerebellar toxicity induced by MTX has not been unclear.

In experimental animals, MTX exposure reportedly induced a toxic effect on the cerebellum in adult guinea pig and rats [8, 47]. Intraperitoneal administration of MTX caused loss, apoptosis and degeneration of Purkinje cells in those animal models [8, 47]. Prenatal MTX exposure reportedly induced developmental anomalies of the cerebellum in chicken embryos [51]. However, there have been no reports to date describing the effect of postnatal exposure to MTX on the cerebellar development of infant animals. In the present study, we carried out a sequential histopathological examination of infant rat cerebellum following MTX administration on postnatal day (PD) 6 for the purpose of elucidating the effect of MTX on cerebellar development in infant rats.

### MATERIALS AND METHODS

**Animals:** Newborn male rats were obtained at Tottori University by mating specific pathogen-free male and female rats of the Wistar Imamichi strain, purchased from the Institute of Animal Reproduction (Kasumigaura, Japan). One mother with 5 male infants were housed together in cages (W335 mm × D380 mm × H175 mm) with bedding (CLEA Japan, Inc., Tokyo, Japan). Because sexual differences in MTX-induced pathological changes in the cerebellum were

\*CORRESPONDENCE TO: SUGIYAMA A., Courses of Veterinary Laboratory Medicine, School of Veterinary Medicine, Faculty of Agriculture, Tottori University, Minami 4-101 Koyama-cho, Tottori, Tottori 680-8553, Japan. e-mail: sugiyama@muses.tottori-u.ac.jp

©2015 The Japanese Society of Veterinary Science

This is an open-access article distributed under the terms of the Creative Commons Attribution Non-Commercial No Derivatives (by-nc-nd) License <<http://creativecommons.org/licenses/by-nc-nd/3.0/>>.

not observed in the preliminary study, male rats were used in the main study.

The animals were reared in a room with the temperature controlled at  $22 \pm 2^\circ\text{C}$ , humidity at  $50 \pm 5\%$ , with ventilation 11 times per hour, lighting at 12:12-hr light/dark cycle (light cycle, 7:00–19:00) and given standard chow (CE-2; Nihon Clea, Tokyo, Japan). The present experiments were performed following the provisions approved by the Animal Research Committee of Tottori University.

**Experimental design:** A total of 60 6-day-old male rats were divided into 2 groups as follows: (1) saline-treated control rats ( $n=30$ ) and (2) MTX-treated rats ( $n=30$ ). MTX (Pfizer Japan Inc., Tokyo, Japan) was dissolved in saline. The 6-day-old rats received intraperitoneal injections (i.p.) with MTX (1 mg/kg body weight) or saline (the control).

Six-day-old male infant rats were treated with 1 mg/kg of MTX, and their brains were sampled from 1, 2, 3, 4, 8 and 15 days after treatment (DAT) to examine the time-course histopathological changes in the cerebellum. The specific timing of MTX administration we used was selected, because the injection of DNA-damaging chemicals such as busulfan, on PD6 induced apoptosis in external granular cells of cerebellum [36]. In our preliminary study, MTX 0.1 mg/kg treatment induced few pathological changes, and MTX 0.5 mg/kg treatment induced quite mild pathological changes in the cerebellum. The dose of MTX in the present study was designated as 1 mg/kg, based on the results of our preliminary study. Rat brain samples were collected under pentobarbital anesthesia (100 mg/kg, i.p.) 1, 2, 3, 4, 8 and 15 days, respectively, after MTX administration. The brain samples were removed from each animal and weighed, and the lengths and widths of the cerebral and cerebellar hemispheres were measured with the digital vernier caliper (Niigata seiki Co., Ltd., Niigata, Japan) according to the previous studies [6, 42, 50].

**Histopathological examination:** All brain samples were fixed in 10% neutral buffered formalin. They were embedded in paraffin, sectioned and stained with hematoxylin and eosin (HE). The number of pyknotic cells or mitotic cells in the external granular layer of lobules VIII–IX of vermis was counted from over 500 external granule cells by light microscopy for each infant animal, and the pyknotic index and mitotic index were calculated as the percentage of pyknotic cells or mitotic cells from out of the total number of external granular cells in lobules VIII–IX of the vermis counted.

**TUNEL method:** DNA-fragmented external granular cells were detected by terminal deoxynucleotidyl-transferase (TdT)-mediated deoxyuridine triphosphate-digoxigenin (dUTP) nick-end labeling (TUNEL), which was performed using an *in situ* apoptosis detection kit (Trevigen, Inc., Gaithersburg, MD, U.S.A.). The number of TUNEL-positive cells in the external granular layer of the lobules VIII–IV of vermis was counted from over 500 external granular cells by light microscopy for each infant animal, and the TUNEL index was calculated as the percentage of TUNEL-positive cells from out of the total number of external granule cells in the lobules VIII–IV of the vermis counted.

**Immunohistochemical examination:** Immunohistochemical staining was performed by a labeled polymer method us-

ing a detection reagent, Histofine Simple Stain MAX-PO (R) (Nichirei, Tokyo, Japan). It is the labeled polymer prepared by combining amino acid polymers with multiple molecules of peroxidase and secondary antibody which is reduced to Fab' fragment. To retrieve the antigen, tissue sections used for the detection of cleaved caspase-3 antigen were immersed in citrate buffer, pH 6.0 (Dako, Glostrup, Denmark) and autoclaved for 15 min at  $121^\circ\text{C}$ ; tissue sections for the detection of phospho-histone H3 antigen and p21 antigen were then immersed in citrate buffer, pH 6.0 (Dako) and microwaved for 15 min. Endogenous peroxidase activity was quenched by immersing the sections in 3% hydrogen peroxide in methanol for 15 min. The sections were incubated with the cleaved caspase-3 rabbit polyclonal antibody (1:300 dilution; Cell Signaling Technology, Inc., Danvers, MA, U.S.A.) or the p21 mouse monoclonal antibody (1:300 dilution; Santa Cruz Biotechnology, Inc., Dallas, TX, U.S.A.) at  $4^\circ\text{C}$  overnight and then were incubated with the phospho-histone H3 rabbit monoclonal antibody (1:1,500 dilution; Abcam, Tokyo, Japan) for 30 min at room temperature. Then, these sections were treated with Histofine Simple Stain MAX-PO (R) (Nichirei) for 30 min at room temperature. They were exposed to a 3,3'-diaminobenzidine solution containing hydrogen peroxide (Nichirei) to facilitate a peroxidase color reaction and then counterstained with Mayer's hematoxylin. The number of cleaved caspase-3-, phospho-histone H3- or p21- positive cells in the external granular layer of lobes VIII–IX of vermis was counted from over 500 external granular cells of each infant animal by light microscopy, and the cleaved caspase-3-, phospho-histone H3- or p21-index was calculated as the percentage of the cleaved caspase-3-, phospho-histone H3- or p21-positive cells out of the total number of external granular cells in lobes VIII–IX of the vermis counted.

**Statistical analysis:** Means  $\pm$  standard error (SE) of the individual litter value was calculated. Comparisons between the 2 groups were made by Student's *t*-test or Welch's *t*-test if data were normally distributed, and by Mann-Whitney *U* test if data were not normally distributed with statistical software ("Excel Toukei 2008", SSRI Co., Ltd., Tokyo, Japan). The data were analyzed with an *F*-test. When variances were homogenous, the Student's *t*-test was performed. Welch's *t*-test was employed when variances were not homogeneous ( $P < 0.05$ ).  $P < 0.05$ ,  $P < 0.01$  or  $P < 0.001$  was considered to be statistically significant.

## RESULTS

**Effects of MTX on infant rats:** No deaths occurred in both groups until 4 DAT. However, mortality on 8 and 15 DAT in the MTX-treated group was 40% and 66.7%, whereas no deaths occurred in the control group on 8 and 15 DAT. Body weight gain of infant rats decreased significantly on 2, 4, 8 and 15 DAT in the MTX-treated group compared with the control group. No abnormal appearance and behavior were observed in any animals, except for dead animals which were depressed before death. The total brain weight decreased significantly in the MTX-treated group compared with the control group from 4 to 15 DAT. The length and width of the

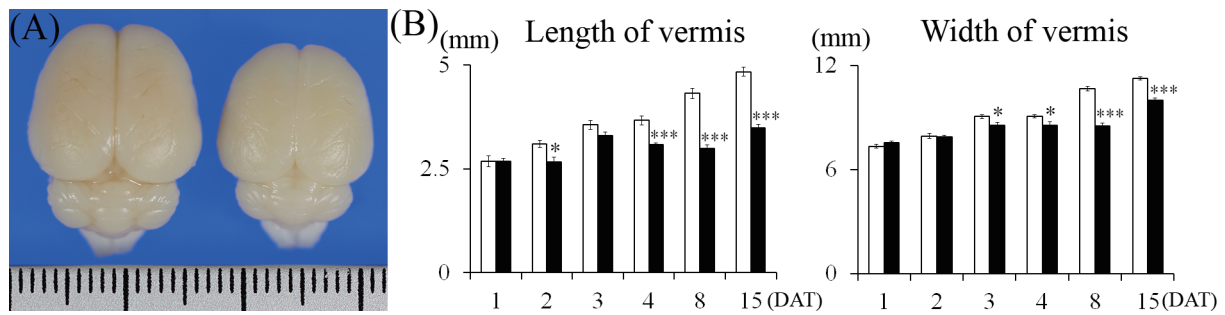


Fig. 1. Dorsal view of rat infant brains on 15 DAT (A) and changes in the length and width of cerebellar vermis (B). (A) Left: Control group. Right: MTX-treated group. The ruler in the figure is graduated in millimeters. (B) □ Control group, ■ MTX-treated group. Values are expressed as means  $\pm$  SE. \*, \*\*\*: Significantly different from control at  $P < 0.05$ ,  $P < 0.001$  (Student's *t*-test).

cerebrum decreased significantly in the MTX-treated group compared with the control group on 8 and 15 DAT.

Cerebellums in the MTX group appeared to be smaller than those in the control group on 15 DAT (Fig. 1A). The length of vermis of the cerebellum decreased significantly in the MTX-treated group, but not in the control on 2, 4, 8 and 15 DAT, and the width of the cerebellum decreased significantly in the MTX-treated group, but not in the control on 3, 4, 8 and 15 DAT (Fig. 1B).

**Histopathological findings:** The size of the cerebellar hemispheres in the MTX-treated group was diminished compared to the control on 15 DAT (Fig. 2). In the control group, few pyknotic changes in external granular cells were observed throughout the experimental period (Figs. 3 and 4A). On 1 DAT, in the MTX group, there were a large number of pyknotic granular cells throughout the external granular layer, and the pyknotic index in the MTX group was significantly higher than in the control group (Figs. 3 and 4A). However, pyknotic cells were sparse in the external granular layer, and the pyknotic index in the MTX group decreased from 3 DAT onward (Figs. 3 and 4A). On the other hand, although there were many mitotic cells in the external granular layer of the control group on 1 DAT, mitotic cells were sparse in the external granular layer of the MTX group. The mitotic index in the external granular layer of MTX group on 1 DAT was significantly lower than in the control group (Fig. 4B). On 2 DAT, the mitotic index in the external granular layer of the MTX group recovered and showed a significant increase on 3 and 4 DAT compared with the control group (Fig. 4B).

The external granular cells decreased on 8 DAT and almost disappeared by 15 DAT in the control group (Figs. 3 and 5A). Moreover, a significant reduction in the width of the external granular layer was detected on 2 and 3 DAT in the MTX group (Figs. 3 and 5A). By 4 DAT, the width of the external granular layer of MTX group increased, and it was greater than the control group's width by 8 DAT (Figs. 3 and 5A). On the other hand, the molecular layer of MTX group on 8 and 15 DAT was significantly thinner than that of the control group (Figs. 3 and 5B).

Most of the pyknotic granular cells were positively stained by the TUNEL method (Fig. 6) and were positive for cleaved

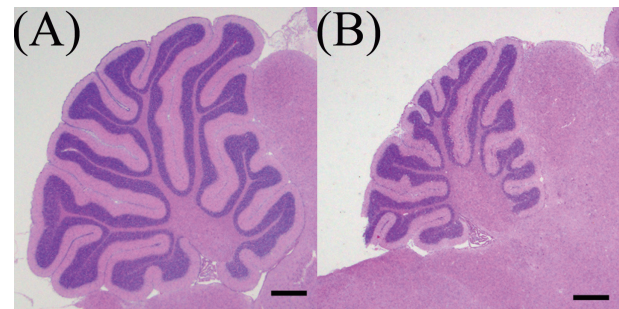


Fig. 2. The size of cerebellar hemispheres in MTX-treated group was diminished compared to a control on 15 DAT. (A) Control group, (B) MTX-treated group. Bar=500  $\mu$ m.

caspase-3 (Fig. 7). On 1 DAT, in the MTX group, TUNEL- and cleaved caspase-3-indices were significantly higher than in the control group, and they decreased from 3 DAT onward (Fig. 8).

On 1 DAT, while there were a large number of phospho-histone H3-positive cells in the external granular layer of the control group, phospho-histone H3-positive cells in the external granular layer of MTX group were sparse, and phospho-histone H3-index was significantly lower than in the control group (Figs. 9 and 11A). On 2 DAT, phospho-histone H3-index of the MTX group recovered and was significantly higher than in the control group (Fig. 11A). Phospho-histone H3-index of the MTX group showed a tendency to increase on 3 and 4 DAT (Fig. 11A).

On 1 DAT, in MTX group, while there were few p21-positive cells in the external granular layer, a large number of p21-positive external granular cells appeared and scattered in the external granular layer (Fig. 10). P21-index in the external layer of MTX group was significantly higher than in the control group on 1–4 DAT, and on 1 DAT, showed a tendency to be higher than the control on 2, 3 and 4 DAT (Fig. 11B).

There were no differences in the density, location and shape of Purkinje cell and the development degree of dendritic spines of Purkinje cells between the control group and MTX group.

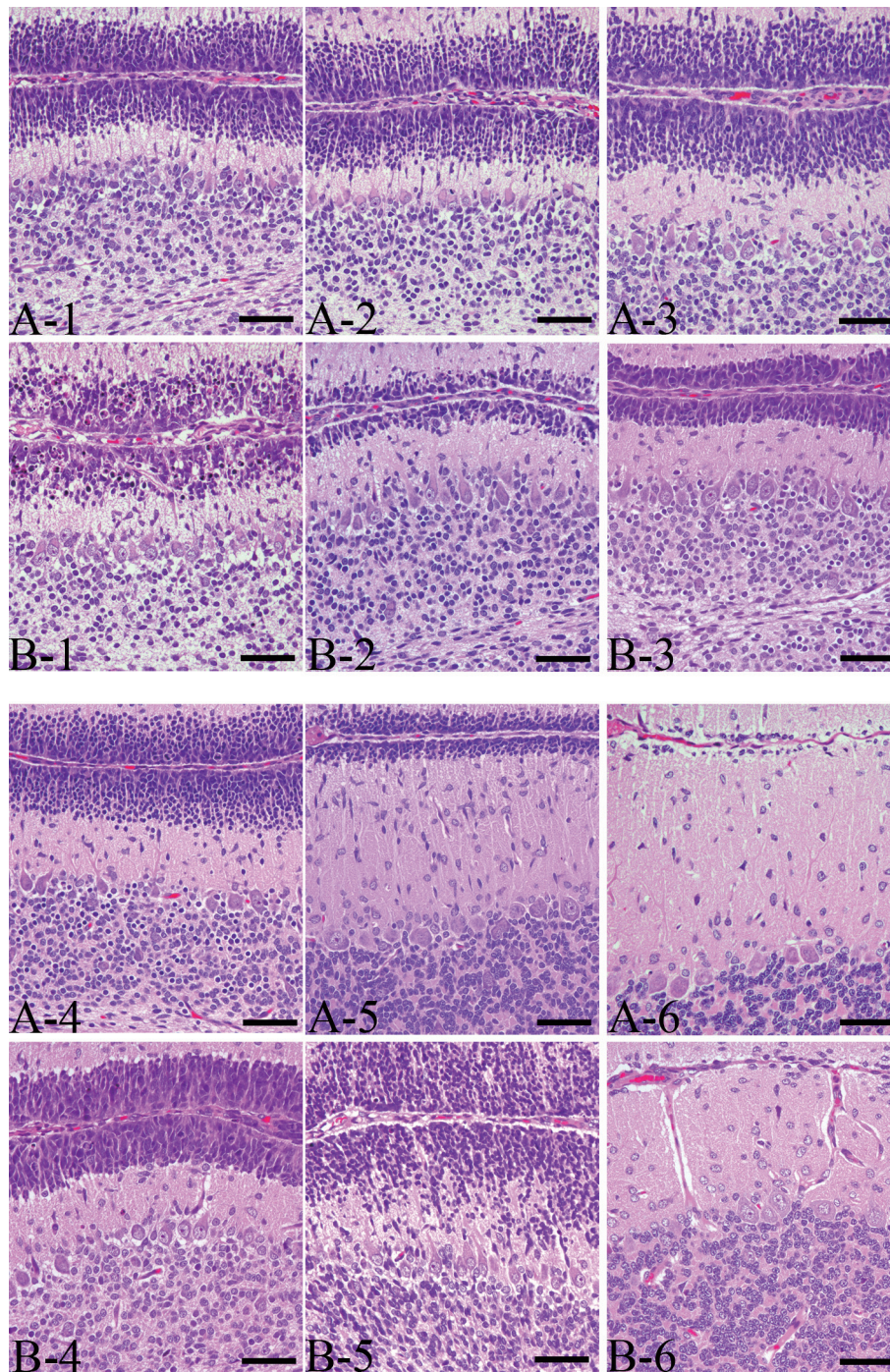


Fig. 3. Sequence of histopathological changes in the external granular cells in the lobules VIII-IV of vermis. (A) Control group, (B) MTX-treated group. Bar=50  $\mu$ m. (1) 1DAT, (2) 2DAT, (3) 3DAT, (4) 4DAT, (5) 8DAT, (6) 15DAT

## DISCUSSION

In the present study, the cerebral and cerebellar length and width in the MTX-treated rats were decreased compared with those of the saline-treated control rats. It was reported that MTX exposure during prenatal period induced microcephaly

in human [2, 20], however, the detailed pathogenesis of MTX-induced microcephaly has been unclarified. To our knowledge, there are no reports about involvement of postnatal MTX exposure in microcephaly. Postnatal MTX exposure reduced cerebral glucose metabolism, and it disrupted the metabolism of dopamine [38, 43]. Postnatal MTX exposure

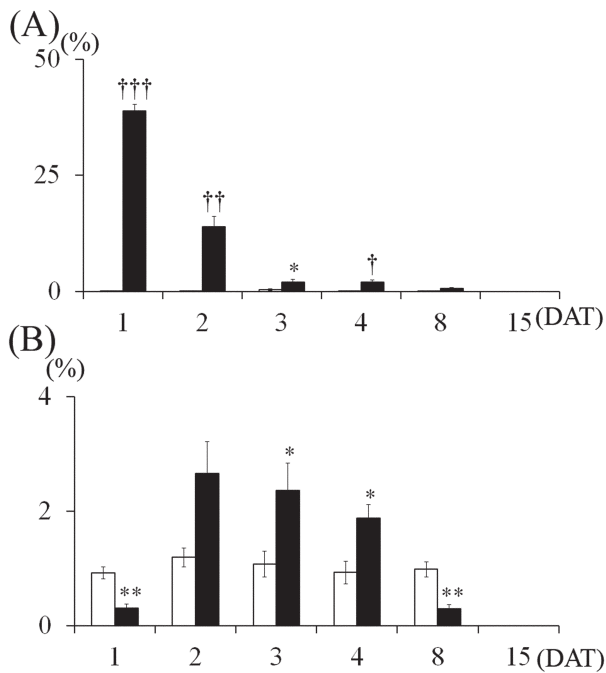


Fig. 4. Changes in pyknotic and mitotic indices of the external granular cells. (A) Pyknotic index, (B) Mitotic index. □ Control group, ■ MTX-treated group. Values are expressed as means  $\pm$  SE. \*, \*\*: Significantly different from control at  $P < 0.05$ ,  $P < 0.01$  (Student's *t*-test). †, ††, †††: Significantly different from control at  $P < 0.05$ ,  $P < 0.01$  and  $P < 0.001$ , respectively (Welch's *t*-test).

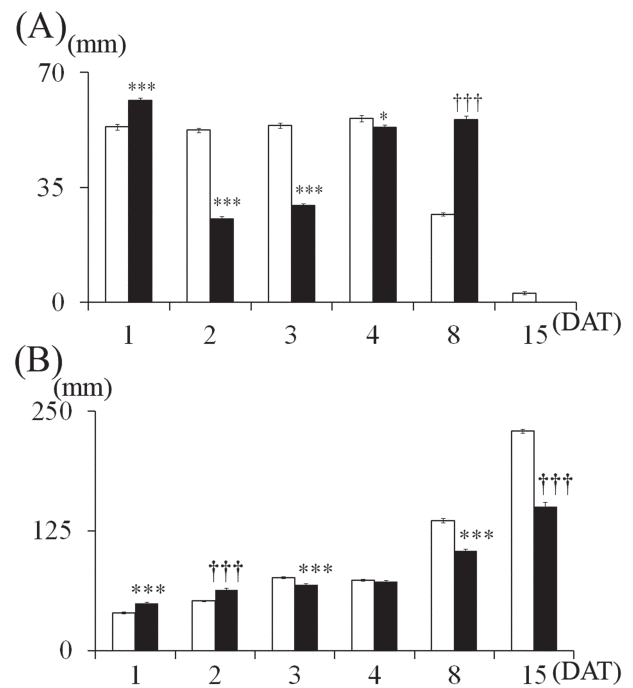


Fig. 5. Changes in the thickness of the external granular layer (A) and molecular layer (B). □ Control group, ■ MTX-treated group. Values are expressed as means  $\pm$  SE. \*, \*\*\*: Significantly different from control at  $P < 0.05$ ,  $P < 0.001$  (Student's *t*-test). †††: Significantly different from control at  $P < 0.001$ , respectively (Welch's *t*-test).

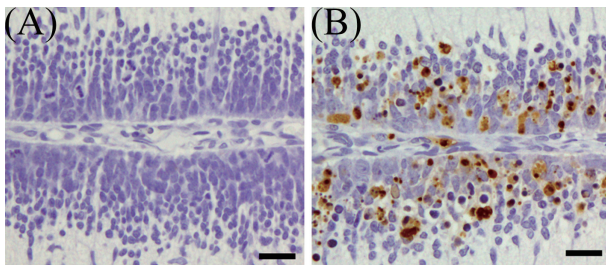


Fig. 6. TUNEL-positive cells in the external granular layer of MTX-treated rat infant cerebellum on 1 DAT. (A) Control group, (B) MTX-treated group. Bar=20  $\mu$ m.

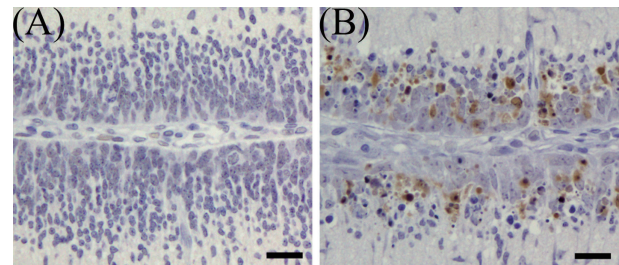


Fig. 7. Immunohistochemical expression of cleaved caspase-3 in the external granular layer of MTX-treated rat infant cerebellum on 1 DAT. (A) Control group, (B) MTX-treated group. Bar=20  $\mu$ m.

decreased cerebral blood flow [31]. These effects of postnatal MTX exposure may be involved with the pathogenesis of miniaturization of the cerebrum observed in the present study.

In the present study, MTX at 1 mg/kg on PD6 induced severe pyknotic changes on the external granular cells on 1DAT. The majority of pyknotic external granular cells were positive for TUNEL staining and cleaved caspase-3. Cleavage of caspase-3 is known to be involved in cell apoptosis and is recognized as an apoptosis marker [13]. These results indicate that pyknotic changes induced by MTX in the present study were caused by apoptosis. In the present study, pyknotic-, TUNEL- and cleaved caspase-3-indices

peaked on 1 DAT and decreased time-dependently. Namely, pyknotic-, TUNEL- and cleaved caspase-3-indices showed single-peaked change. Although there are several mechanisms of apoptosis by MTX [17, 23, 33, 45], apoptosis may be caused by a single mechanism in the present study.

In the present study, MTX treatment on PD6 induced significant decrease of phospho-Histone H3-positive external granular cells on 1 DAT. Histone H3, a protein involved in chromatin structure, is phosphorylated at serine 10 during chromatin condensation in mitosis [16]. The present result suggests that MTX exposure on PD 6, suppresses cell proliferation in the external granular layer. On PD 6 in the control

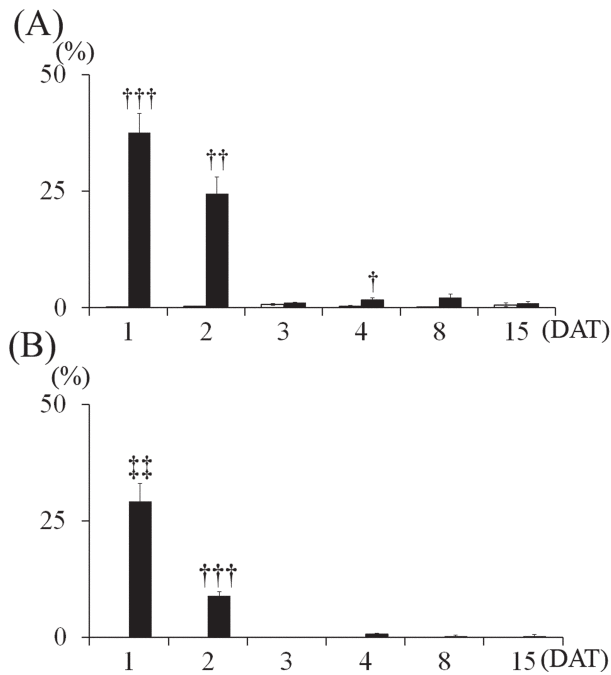


Fig. 8. Changes in TUNEL- and cleaved caspase-3-indices in the external granular cells. (A) TUNEL-index, (B) Cleaved caspase-3-index. □ Control group, ■ MTX-treated group. Values are expressed as means  $\pm$  SE. †, ††, †††: Significantly different from control at  $P < 0.05$ ,  $P < 0.01$  and  $P < 0.001$ , respectively (Welch's *t*-test). ‡, ‡‡: Significantly different from control at  $P < 0.01$  (Mann-Whitney's *U*-test).

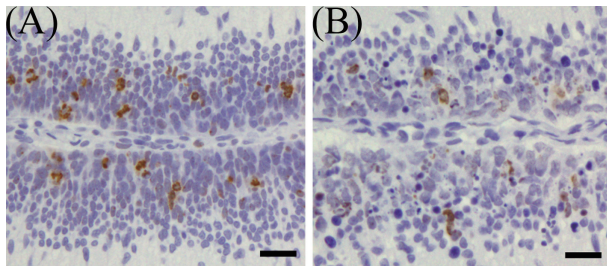


Fig. 9. Immunohistochemical expression of phospho-histone H3 in the external granular layer of rat infant cerebellum on 1 DAT. (A) Control group, (B) MTX-treated group. Bar=20  $\mu$ m.

group, a large number of phospho-Histone H3-positive cells were observed in the external granular layer of cerebellum. These histopathological findings suggest that active cell proliferation occurs in the external granular layer on PD 6 in rats. It was reported that active cell proliferation is observed in the external granular layer by PD 13 in rats [36].

In the present study, while the external granular layer thickness of VIII-IX lobules of vermis in the control group decreased after 8 DAT, the external granular layer thickness of the MTX group decreased significantly on 2 and 3 DAT. It was considered that the significant decrease in external

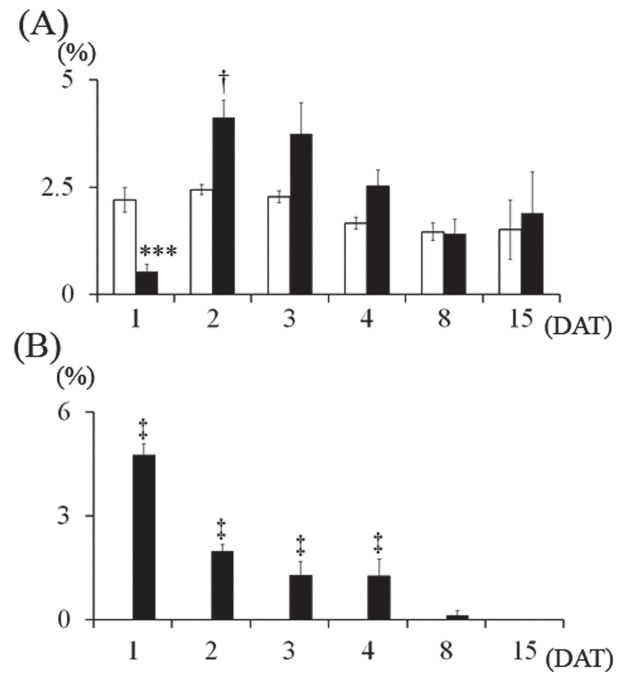


Fig. 11. Changes in Phospho-Histone H3- and p21-indices in the external granular cells. (A) Phospho-Histone H3-index, (B) P21-index. □ Control group, ■ MTX-treated group. Values are expressed as means  $\pm$  SE. \*\*\*: Significantly different from control at  $P < 0.001$  (Student's *t*-test). †: Significantly different from control at  $P < 0.05$  (Welch's *t*-test). ‡: Significantly different from control at  $P < 0.05$  (Mann-Whitney's *U*-test).

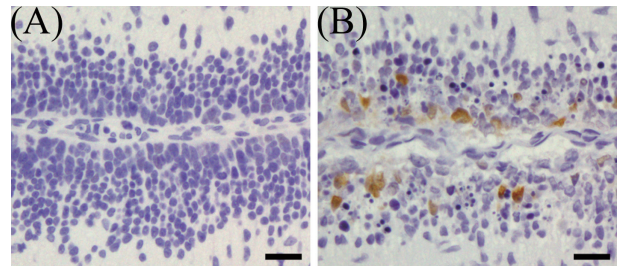


Fig. 10. Immunohistochemical expression of p21 in the external granular layer of rat infant cerebellum on 1 DAT. (A) Control group, (B) MTX-treated group. Bar=20  $\mu$ m.

granular layer thickness at these time points in the MTX group could be attributed to inhibition in the production of external granular cells that had arisen from apoptosis and the decrease in cell proliferative activity. The external granular layer thickness of the MTX group recovered on 4 DAT and was thicker than that of the control group on 8 DAT. These results demonstrated that MTX exposure on PD6 induced a delay, slowing the migration of the external granular cell to the inner granular layer. A previous study suggested that 2 Gy irradiation on PD6 caused a delay in the migration of the external granular cells to the inner granular layer in the

mouse cerebellum [19].

In the axon of the granular cells, the parallel fiber establishes synapses with the spines of spiny dendrites of the Purkinje cells [48]. A previous study suggested that the inhibition of granular cell production may induce developmental disorders in the spiny dendrites of Purkinje cell, such as the downward directed spiny dendrites of the T-shaped Purkinje cells and the low-density dendrites in Purkinje cells [48]. In the present study, thinning of the molecular layer in the MTX group may be attributed to incomplete development of the parallel fiber and spiny dendrites of the Purkinje cells, which are principal components of the molecular layer [15], induced by MTX.

In the present study, MTX treatment significantly increased levels of p21-index and decreased levels of mitotic- and phospho-histone H3-indices on 1 DAT. A moderate inverse correlation was observed between time-dependent movement of the p21-index and that of mitotic- and phospho-histone H3-indices. Several previous studies have shown that MTX induced p21 expression [7, 14, 18, 44]. Western blot analysis revealed that MTX induced p21 protein expression in human adenocarcinoma cells or human breast cancer cells [7, 14]. Flow cytometry analysis with human T cells showed that MTX treatment significantly increased levels of p21 [44]. RT-PCR demonstrated that MTX induced p21 gene expression in human lung carcinoma cells [18]. P21 is a member of cyclin-dependent kinase (CDK) inhibitors, which negatively modulates cell cycles by inhibiting the activity of CDK in a complex with cyclin [26, 40, 45]. P21 induces cell cycle arrest in the G1 or G2 phase after DNA damage [3, 4]. It was suggested that decrease of the mitotic- and phospho-histone H3-index in the present study could be attributed to cell cycle arrest induced by p21. P21 is a downstream transcriptional target of p53 and was induced in wild-type p53-containing cells by exposure to DNA damaging agents [9]. Doxorubicin and busulfan are known as DNA damaging agents [36, 37]. Western blot analysis demonstrated that doxorubicin up-regulated the protein expression of p53 and p21 in mouse cerebellar granule cells [37]. Immunohistochemical analysis revealed busulfan increased the number of p53- and p21-positive cells in the external granular cells of infant rats [36]. Previous studies showed that MTX induces not only inhibition of DNA synthesis but also DNA damage [25, 28]. In the present study, p21 expression may have been induced by p53 expression after DNA damage. In a previous study, flow cytometry analysis with human T cells revealed that MTX treatment induced expression of both p53 and p21 by JNK-2- and JNK-1-dependent mechanisms [44].

A previous study showed that a single intraperitoneal dose of MTX 20 mg/kg caused loss, apoptosis and degeneration of Purkinje cells relevant to oxidative stress in adult Wistar rats [47]. In the present study, obvious pathological changes of Purkinje cell were not observed in cerebellum of the MTX group. These results may be attributed to the difference in dosage.

A previous study demonstrated that MTX is excreted into breast milk [21]. It was detectable in breast milk 2 hr after administration to a woman treated with MTX 22.5 mg/kg/

day for choriocarcinoma, and the MTX level in milk reached a peak between 4 and 10 hr later at an 8% concentration of the plasma concentration [21]. MTX is a highly ionized and lipid-insoluble compound that barely penetrates the blood-brain barrier [12]. However, several previous studies demonstrated that intravenous or oral administration of MTX induced central nervous system toxicity [1, 12, 39, 49]. Furthermore, the blood-brain barrier develops to acquire the barrier function and protect the brain from neurotoxic substances [46]. The infant brain is vulnerable to neurotoxic substances due to the immature blood-brain barrier [41, 46]. Because it is possible that MTX treatment in the lactation period causes some adverse effect on cerebellar development in infant, breastfeeding during MTX administration should be avoided.

It was reported that MTX chemotherapy and cranial irradiation induced cerebellar hypoplasia in children with ALL at age 2–5 years [5]. Because the external granular layer of human cerebellum is detectable until an age of 1 year [10], it is considered that the pathogenesis of cerebellar hypoplasia in children induced by MTX chemotherapy and irradiation is not involved with damage of the external granular cells. Cerebellar hypoplasia associated with damage of the external granular cell in rats was induced by cytarabine 30 or 50 mg/kg 2, 3 and 4 days after birth [42].

In conclusion, MTX administration of 1 mg/kg on PD6 induced apoptosis of external granular cells and inhibited their proliferation, causing migratory delay of those cells and resulting in cerebellar hypoplasia. It was suggested that inhibition of cell proliferation activity of the external granule cells was mediated by p21 expression induced by MTX. While the detailed molecular mechanisms of MTX-induced apoptosis in the external granular cells remain unclear, the results of the present study provide fundamental information about cerebellar hypoplasia induced by MTX. To our knowledge, this is the first report demonstrating histopathological findings of cerebellar developmental disorder induced by MTX.

## REFERENCES

1. Allen, J. C., Thaler, H. T., Deck, M. D. and Rottenberg, D. A. 1978. Leukoencephalopathy following high-dose intravenous methotrexate chemotherapy: quantitative assessment of white matter attenuation using computed tomography. *Neuroradiology* **16**: 44–47. [Medline] [CrossRef]
2. Bawle, E. V., Conard, J. V. and Weiss, L. 1998. Adult and two children with fetal methotrexate syndrome. *Teratology* **57**: 51–55. [Medline] [CrossRef]
3. Brugarolas, J., Moberg, K., Boyd, S. D., Taya, Y., Jacks, T. and Lees, J. A. 1999. Inhibition of cyclin-dependent kinase 2 by p21 is necessary for retinoblastoma protein-mediated G1 arrest after gamma-irradiation. *Proc. Natl. Acad. Sci. U.S.A.* **96**: 1002–1007. [Medline] [CrossRef]
4. Bunz, F., Dutriaux, A., Lengauer, C., Waldman, T., Zhou, S., Brown, J. P., Sedivy, J. M., Kinzler, K. W. and Vogelstein, B. 1998. Requirement for p53 and p21 to sustain G2 arrest after DNA damage. *Science* **282**: 1497–1501. [Medline] [CrossRef]
5. Ciesielski, K. T., Yanofsky, R., Ludwig, R. N., Hill, D. E., Hart,

- B. L., Astur, R. S. and Snyder, T. 1994. Hypoplasia of the cerebellar vermis and cognitive deficits in survivors of childhood leukemia. *Arch. Neurol.* **51**: 985–993. [Medline] [CrossRef]
6. Cooper, G. M., Mooney, M. P., Burrows, A. M., Smith, T. D., Dechant, J., Losken, H. W., Marsh, J. L. and Siegel, M. I. 1999. Brain growth rates in craniosynostotic rabbits. *Cleft Palate Craniofac. J.* **36**: 314–321. [Medline] [CrossRef]
7. Dabrowska, M., Mosieniak, G., Skierski, J., Sikora, E. and Rode, W. 2009. Methotrexate-induced senescence in human adenocarcinoma cells is accompanied by induction of p21(waf1/cip1) expression and lack of polyploidy. *Cancer Lett.* **284**: 95–101. [Medline] [CrossRef]
8. el-Badawi, M. G., Fatani, J. A., Bahakim, H. and Abdalla, M. A. 1990. Light and electron microscopic observations on the cerebellum of guinea pigs following low-dose methotrexate. *Exp. Mol. Pathol.* **53**: 211–222. [Medline] [CrossRef]
9. el-Deiry, W. S., Harper, J. W., O'Connor, P. M., Velculescu, V. E., Canman, C. E., Jackman, J., Pietenpol, J. A., Burrell, M., Hill, D. E., Wang, Y., Wiman, K. G., Edward Mercer, W., Kastan, M. B., Kohn, K. W., Ellenge, S. J., Kinzler, K. W. and Vogelstein, B. 1994. WAF1/CIP1 is induced in p53-mediated G1 arrest and apoptosis. *Cancer Res.* **54**: 1169–1174. [Medline]
10. Gelpi, E., Budka, H. and Preusser, M. 2013. External granular cell layer bobbling: a distinct histomorphological feature of the developing human cerebellum. *Clin. Neuropathol.* **32**: 42–50. [Medline] [CrossRef]
11. Genestier, L., Paillot, R., Quemeneur, L., Izeradjene, K. and Revillard, J. P. 2000. Mechanisms of action of methotrexate. *Immunopharmacology* **47**: 247–257. [Medline] [CrossRef]
12. González-Suárez, I., Aguilar-Amat, M. J., Trigueros, M., Borobia, A. M., Cruz, A. and Arpa, J. 2014. Leukoencephalopathy due to oral methotrexate. *Cerebellum* **13**: 178–183. [Medline] [CrossRef]
13. Gown, A. M. and Willingham, M. C. 2002. Improved detection of apoptotic cells in archival paraffin sections: immunohistochemistry using antibodies to cleaved caspase 3. *J. Histochem. Cytochem.* **50**: 449–454. [Medline] [CrossRef]
14. Hattangadi, D. K., DeMasters, G. A., Walker, T. D., Jones, K. R., Di, X., Newsham, I. F. and Gewirtz, D. A. 2004. Influence of p53 and caspase 3 activity on cell death and senescence in response to methotrexate in the breast tumor cell. *Biochem. Pharmacol.* **68**: 1699–1708. [Medline] [CrossRef]
15. Heinsen, H. and Heinsen, Y. L. 1983. Quantitative studies on regional differences in Purkinje cell dendritic spines and parallel fiber synaptic density. *Anat. Embryol. (Berl.)* **168**: 361–370. [Medline] [CrossRef]
16. Hendzel, M. J., Wei, Y., Mancini, M. A., Van Hooser, A., Ranalli, T., Brinkley, B. R., Bazett-Jones, D. P. and Allis, C. D. 1997. Mitosis-specific phosphorylation of histone H3 initiates primarily within pericentromeric heterochromatin during G2 and spreads in an ordered fashion coincident with mitotic chromosome condensation. *Chromosoma* **106**: 348–360. [Medline] [CrossRef]
17. Herman, S., Zurgil, N. and Deutsch, M. 2005. Low dose methotrexate induces apoptosis with reactive oxygen species involvement in T lymphocytic cell lines to a greater extent than in monocytic lines. *Inflamm. Res.* **54**: 273–280. [Medline] [CrossRef]
18. Huang, W. Y., Yang, P. M., Chang, Y. F., Marquez, V. E. and Chen, C. C. 2011. Methotrexate induces apoptosis through p53/p21-dependent pathway and increases E-cadherin expression through downregulation of HDAC/EZH2. *Biochem. Pharmacol.* **81**: 510–517. [Medline] [CrossRef]
19. Hyodo-Taguchi, Y., Fushiki, S., Kinoshita, C., Ishikawa, Y. and Hirobe, T. 1998. Effects of low-dose X-irradiation on the development of the mouse cerebellar cortex. *J. Radiat. Res. (Tokyo)* **39**: 11–19. [Medline] [CrossRef]
20. Hyoun, S. C., Običan, S. G. and Scialli, A. R. 2012. Teratogen update: methotrexate. *Birth Defects Res. A Clin. Mol. Teratol.* **94**: 187–207. [Medline] [CrossRef]
21. Johns, D. G., Rutherford, L. D., Leighton, P. C. and Vogel, C. L. 1972. Secretion of methotrexate into human milk. *Am. J. Obstet. Gynecol.* **112**: 978–980. [Medline]
22. Jolivet, J., Cowan, K. H., Curt, G. A., Clendeninn, N. J. and Chabner, B. A. 1983. The pharmacology and clinical use of methotrexate. *N. Engl. J. Med.* **309**: 1094–1104. [Medline] [CrossRef]
23. Kobayashi, K., Terada, C. and Tsukamoto, I. 2002. Methotrexate-induced apoptosis in hepatocytes after partial hepatectomy. *Eur. J. Pharmacol.* **438**: 19–24. [Medline] [CrossRef]
24. Lesnik, P. G., Ciesielski, K. T., Hart, B. L., Benzel, E. C. and Sanders, J. A. 1998. Evidence for intrathecal chemotherapy for leukemia. *Arch. Neurol.* **55**: 1561–1568. [Medline] [CrossRef]
25. Li, J. C. and Kaminskas, E. 1984. Accumulation of DNA strand breaks and methotrexate cytotoxicity. *Proc. Natl. Acad. Sci. U.S.A.* **81**: 5694–5698. [Medline] [CrossRef]
26. Liu, S., Bishop, W. R. and Liu, M. 2003. Differential effects of cell cycle regulatory protein p21 (WAF1/Cip1) on apoptosis and sensitivity to cancer chemotherapy. *Drug Resist. Updat.* **6**: 183–195. [Medline] [CrossRef]
27. Lloyd, M. E., Carr, M., McElhatton, P., Hall, G. M. and Hughes, R. A. 1999. The effects of methotrexate on pregnancy, fertility and lactation. *QJM* **92**: 551–563. [Medline] [CrossRef]
28. Lorico, A., Toffoli, G., Boiocchi, M., Erba, E., Broggin, M., Rappa, G. and D'Incalci, M. 1988. Accumulation of DNA strand breaks in cells exposed to methotrexate or N10-propargyl-5,8-dideazafolic acid. *Cancer Res.* **48**: 2036–2041. [Medline]
29. Margolis, S., Philips, F. S. and Sternberg, S. S. 1971. The cytotoxicity of methotrexate in mouse small intestine in relation to inhibition of folic acid reductase and of DNA synthesis. *Cancer Res.* **31**: 2037–2046. [Medline]
30. Masterson, K., Merlini, L. and Lövblad, K. O. 2009. Coexistence of reversible cerebral neurotoxicity and irreversible cerebellar atrophy following an intrathecal methotrexate chemotherapy: two case reports. *J. Neuroradiol.* **36**: 112–114. [Medline] [CrossRef]
31. Mizusawa, S., Kondoh, Y., Murakami, M., Nakamichi, H., Sasaki, H., Komatsu, K., Takahashi, A., Kudoh, Y., Watanabe, K., Ono, Y. and Uemura, K. 1988. Effect of methotrexate on local cerebral blood flow in conscious rats. *Jpn. J. Pharmacol.* **48**: 499–501. [Medline] [CrossRef]
32. Mori, T., Fukano, R., Saito, A., Takimoto, T., Sekimizu, M., Nakazawa, A., Tsurusawa, M., Kobayashi, R. and Horibe, K. 2014. Japanese Pediatric Leukemia/Lymphoma Study Group. Analysis of Japanese registration from the randomized international trial for childhood anaplastic large cell lymphoma (ALCL99-R1). *Rinsho Ketsueki* **55**: 526–533. [Medline]
33. Müller, M., Strand, S., Hug, H., Heinemann, E. M., Walczak, H., Hofmann, W. J., Stremmel, W., Krammer, P. H. and Galle, P. R. 1997. Drug-induced apoptosis in hepatoma cells is mediated by the CD95 (APO-1/Fas) receptor/ligand system and involves activation of wild-type p53. *J. Clin. Invest.* **99**: 403–413. [Medline] [CrossRef]
34. Nomura, M., Narita, Y., Miyakita, Y., Ohno, M., Fukushima, S., Maruyama, T., Muragaki, Y. and Shibui, S. 2013. Clinical

- presentation of anaplastic large-cell lymphoma in the central nervous system. *Mol. Clin. Oncol.* **1**: 655–660. [Medline]
35. Ogungbenro, K., Aarons, L. and CRESim & Epi-CRESim Project Groups. 2014. Physiologically based pharmacokinetic modelling of methotrexate and 6-mercaptopurine in adults and children. Part 1: methotrexate. *J. Pharmacokinet. Pharmacodyn.* **41**: 159–171. [Medline] [CrossRef]
  36. Ohira, T., Ando, R., Saito, T., Yahata, M., Oshima, Y. and Tamura, K. 2013. Busulfan-induced pathological changes of the cerebellar development in infant rats. *Exp. Toxicol. Pathol.* **65**: 789–797. [Medline] [CrossRef]
  37. Otsuka, Y., Tanaka, T., Uchida, D., Noguchi, Y., Saeki, N., Saito, Y. and Tatsuno, I. 2004. Roles of cyclin-dependent kinase 4 and p53 in neuronal cell death induced by doxorubicin on cerebellar granule neurons in mouse. *Neurosci. Lett.* **365**: 180–185. [Medline] [CrossRef]
  38. Phillips, P. C., Thaler, H. T., Berger, C. A., Fleisher, M., Wellner, D., Allen, J. C. and Rottenberg, D. A. 1986. Acute high-dose methotrexate neurotoxicity in the rat. *Ann. Neurol.* **20**: 583–589. [Medline] [CrossRef]
  39. Reddick, W. E., Glass, J. O., Helton, K. J., Langston, J. W., Xiong, X., Wu, S. and Pui, C. H. 2005. Prevalence of leukoencephalopathy in children treated for acute lymphoblastic leukemia with high-dose methotrexate. *AJNR Am. J. Neuroradiol.* **26**: 1263–1269. [Medline]
  40. Roninson, I. B. 2002. Oncogenic functions of tumour suppressor p21 (Waf1/Cip1/Sdi1): association with cell senescence and tumour-promoting activities of stromal fibroblasts. *Cancer Lett.* **179**: 1–14. [Medline] [CrossRef]
  41. Saunders, N. R., Habgood, M. D. and Dziegielewska, K. M. 1999. Barrier mechanisms in the brain, II. Immature brain. *Clin. Exp. Pharmacol. Physiol.* **26**: 85–91. [Medline] [CrossRef]
  42. Shimada, M., Wakaizumi, S., Kasubuchi, Y. and Kusonoki, T. 1975. Cytarabine and its effect on cerebellum of suckling mouse. *Arch. Neurol.* **32**: 555–559. [Medline] [CrossRef]
  43. Silverstein, F. S. and Johnston, M. V. 1986. A model of methotrexate encephalopathy: neurotransmitter and pathologic abnormalities. *J. Child Neurol.* **1**: 351–357. [Medline] [CrossRef]
  44. Spurlock, C. F. 3rd., Tossberg, J. T., Fuchs, H. A., Olsen, N. J. and Aune, T. M. 2012. Methotrexate increases expression of cell cycle checkpoint genes via JNK activation. *Arthritis Rheum.* **64**: 1780–1789. [Medline] [CrossRef]
  45. Stivala, L. A., Cazzalini, O. and Prosperi, E. 2012. The cyclin-dependent kinase inhibitor p21<sup>CDKN1A</sup> as a target of anti-cancer drugs. *Curr. Cancer Drug Targets* **12**: 85–96. [Medline] [CrossRef]
  46. Takata, F., Dohgu, S., Yamauchi, A., Matsumoto, J., Machida, T., Fujishita, K., Shibata, K., Shinozaki, Y., Sato, K., Kataoka, Y. and Koizumi, S. 2013. *In vitro* blood-brain barrier models using brain capillary endothelial cells isolated from neonatal and adult rats retain age-related barrier properties. *PLoS ONE* **8**: e55166. [Medline] [CrossRef]
  47. Vardi, N., Parlakpinar, H. and Ates, B. 2012. Beneficial effects of chlorogenic acid on methotrexate-induced cerebellar Purkinje cell damage in rats. *J. Chem. Neuroanat.* **43**: 43–47. [Medline] [CrossRef]
  48. Yamano, T., Shimada, M., Abe, Y., Ohta, S. and Ohno, M. 1983. Destruction of external granular layer and subsequent cerebellar abnormalities. *Acta Neuropathol.* **59**: 41–47. [Medline] [CrossRef]
  49. Yokoo, H., Nakazato, Y., Harigaya, Y., Sasaki, N., Igeta, Y. and Itoh, H. 2007. Massive myelinolytic leukoencephalopathy in a patient medicated with low-dose oral methotrexate for rheumatoid arthritis: an autopsy report. *Acta Neuropathol.* **114**: 425–430. [Medline] [CrossRef]
  50. Yoshizawa, K., Emoto, Y., Kinoshita, Y., Yuri, T. and Tsubura, A. 2013. N-methyl-N-nitrosourea-induced cerebellar hypoplasia in rats: Effect of arachidonic acid supplementation during the gestational, lactational and post-weaning periods. *Exp. Ther. Med.* **6**: 627–634. [Medline]
  51. Zamenhof, S. 1985. Differential effects of antifolate on the development of brain parts in chick embryos. *Growth* **49**: 28–33. [Medline]